


CONTENTS

ABSTRACT (CHINESE)	i
ABSTRACT (ENGLISH)	iii
ACKNOWLEDGEMENTS	v
CONTENTS	vi
TABLE CAPTIONS	viii
FIGURE CAPTIONS	ix
TABLE FOR FULL TEXT OF CHEMICAL REAGENTS	xiv
	
CHAPTER1 INTRODUCTION	
1.1 BACKGROUND	1
1.2 REVIEWS ON NANODEVICES	5
1.3 MOTIVATIONS	9
1.4 THESIS ORGANIZATION	10
CHAPTER2 THE CHARACTERISTICS OF NANODEVICE AND CMOS SENSING CHIP	
2.1 THE OPTICAL AND ELECTRICAL PROPERTIES OF Au AND CdSe/ZnS NANOPARTICLES	20
2.2 REVIEW ON Tyramine-CdSe / Au NANODEVICE	23
2.3 THE OPERATIONAL PRINCIPLES OF CMOS SENSING CHIP	27

**CHAPTER3 FABRICATION TECHNOLOGIES OF CdSe/ZnS /
Au NANOPARTICLES AND NANODEVICE**

3.1 THE SYNTHESIS OF Citrate-Capped Au NANOPARTICLES	38
3.2 THE SYNTHESIS OF AET-Capped AND MSA-Capped CdSe/ZnS NANOPARTICLES	38
3.3 THE ASSEMBLY OF Au / AET-CdSe/ZnS AND MSA-CdSe/ZnS / AET-CdSe/ZnS ON SILICON OXIDE SUBSTRATE BY IONIC INTERACTION	40

**CHAPTER4 THE EXPERIMENTAL RESULTS AND
DISCUSSIONS**

4.1 THE ENVIRONMENT SETUP FOR MEASUREMENT	51
4.2 SEM AND OPTICAL ABSORPTION / EMISSION SPECTRA	53
4.3 Au / AET-CdSe/ZnS NANODEVICE	56
4.4 MSA-CdSe/ZnS / AET-CdSe/ZnS NANODEVICE	59
4.5 Au / AET-CdSe/ZnS SOLAR CELL EFFICIENCY	60
4.6 THE PHOTO-SENSING CIRCUIT	62

CHAPTER5 CONCLUSIONS AND FUTURE WORKS

5.1 CONCLUSIONS	103
5.2 FUTURE WORKS	105
REFERENCE	108
VITA	110

TABLE CAPTIONS

CHAPTER 2

Table. 2.1 The voltage biases of CMOS sensing circuit for simulation results.

CHAPTER 4

Table. 4.1 The measurement results of short-circuit current I_{sc} , open-circuit voltage V_{oc} , and photocurrent volume density (PVD) ratio of Au / AET-CdSe/ZnS, multi-layered nanodevice.

Table. 4.2 The simulation results of multi-layers, two-dimensional nano-Schottky-diode arrays model by using HSPICE software.

Table. 4.3 The measurement results of short-circuit current I_{sc} , and photocurrent volume density (PVD) ratio of MSA-CdSe/ZnS / AET-CdSe/ZnS, multi-layered nanodevice.

Table. 4.4 The measurement conditions for measure the Au / AET-CdSe/ZnS, 4-layered nanodevice, $30\mu\text{m} * 5\mu\text{m}$ electrodes combined with CMOS sensing circuit.

FIGURE CAPTIONS

CHAPTER 1

- Fig. 1.1** Chemistry is the central science for further applications such as material science and biotechnology. The combination of advanced materials and tailored biomolecules will produce the future nanodevices [1].
- Fig. 1.2** A gap currently exists in the engineering of small-scale devices. The top-down processes will have their limit below 100 nm, and the bottom-up processes will also have a limit at 2~5 nm. The gap will be filled by nanoclusters and biomolecules [1].
- Fig. 1.3** The TEM images of SiO₂@Au NP clusters synthesized at (A) pH=8.4, (B) pH=8.6, (C) pH=10.2, (D) pH=11.1. The scale bar for all micrographs is 200 nm [2].
- Fig. 1.4** The TEM images of SiO₂@CdSe NP clusters synthesized at (A) pH=6.8, (B) pH=7.2, (C) pH=10.2, (D) pH=11.1. The scale bar for all micrographs is 100 nm [2].
- Fig. 1.5** (a) The schematic diagram of trapping NPs in a submicron narrow gap (5 μm * 5 μm * 1 μm) and a submicron sized light source. (b) The fabrication process of a submicron sized light source based on SOI and CdSe/ZnS NPs [16].
- Fig. 1.6** (A) Optical microscope image of Au-Ppy-Au rods. (B) Optical microscope image of Au-Ppy-Au rods. The lower left inset shows the corresponding FESEM image [17].
- Fig. 1.7** The measurement results of I-V characteristics. (A) For the gold blocks (1-2, 3-4) within a single nanorod at room temperature. Inset shows the optical microscope image (1000 magnification) of a single Au-Ppy-Au rod on microelectrodes. (B) Temperature-dependent I-V curves for measurements across electrodes 2 and 3. (C) For a single Au-Ppy-Cd-Au rod at room temperature [17].
- Fig. 1.8** The efficiency evolution of best research cells by several of technology types. This table identifies those cells that have been measured under standard conditions and confirmed at one of the world's accepted centers for standard solar-cell measurements [18].
- Fig. 1.9** (a) Linking CdSe QDs to TiO₂ particles with bifunctional surface modifier (HS-R-COOH); (b) Light harvesting assembly composed of TiO₂ film functionalized with CdSe QDs on Optically Transparent Electrode (OTE) [19]. (Not to scale)
- Fig. 1.10** The sequence of steps for linking CdSe QDs to TiO₂ surface with a bifunctional surface modifier [19].
- Fig. 1.11** I-V characteristics of (a) OTE/TiO₂ and (b) OTE/TiO₂/MPA/CdSe films. The filtered lights allowed excitation of TiO₂ and CdSe films at wavelengths greater than 300 and 400 nm, respectively [19].

CHAPTER 2

- Fig. 2.1** Density of states in metal (A) and semiconductor (B) nanocrystals. In each case, the density of states is discrete at the band edges. The Fermi level is in the center of a band in a metal, and so kT will exceed the level spacing even at low temperature and small size. In semiconductor, the Fermi level lies between two bands, so that there is large level spacing even at large size. The HOMO-LUMO gap increases as the semiconductor nanocrystals of smaller size (below 10 nm) [11].
- Fig. 2.2** (a) Illustration of a STM tip-single metal NP-insulator coated gold substrate double tunnel junction and corresponding equivalent circuit. (b) Current versus voltage for a single galvanol-coated Au NP acquired in aqueous solution at pH 5. Inset shows an STM image of the sample. Tip was coated with Apiezon wax and gold substrate was coated with hexanethiol [8].
- Fig. 2.3** SEM images of (a)-(e) 50k magnification and (f)-(j) 150k magnification. (a) (f) Au NPs / SiO₂ (Au NPs assembled on SiO₂ substrate), (b) (g) CdSe NPs / Au NPs / SiO₂, (c) (h) Au NPs / CdSe NPs / Au NPs / SiO₂, (d) (i) CdSe NPs / Au NPs / CdSe NPs / Au NPs / SiO₂, and (e) (j) Au NPs / CdSe NPs / Au NPs / CdSe NPs / Au NPs / SiO₂. Note that for better resolution, 3 nm thickness of Pt was plated on each sample prior to SEM performing [14].
- Fig. 2.4** The close photographs of SiO₂/Si wafer fragments of different level assembly process. (right 1) blank SiO₂/Si wafer fragment. (right 2) Au NPs on SiO₂/Si wafer fragment. (right 3) CdSe NPs + Au NPs on SiO₂/Si wafer fragment. (right 4) Au NPs + CdSe NPs + Au NPs on SiO₂/Si wafer fragment. (right 5) CdSe NPs + Au NPs + CdSe NPs + Au NPs on SiO₂/Si wafer fragment. (right 6) Au NPs + CdSe NPs + Au NPs + CdSe NPs + Au NPs on SiO₂/Si wafer fragment [14].
- Fig. 2.5** The images of the electrodes at different stages. (a) Optical microscope image of the silicon chip. (b) (c) SEM images of the two types of electrodes of size 30 μm / 15 μm and 30 μm / 5 μm (width / length). (d) (e) The larger magnification of the edge part of the electrodes after fabrication of a layer of Au NPs (Au NPs / SiO₂) and the 4-layered structure (CdSe NPs / Au NPs / CdSe NPs / Au NPs / SiO₂) [14].
- Fig. 2.6** The measurement results of the nanodevice with and without illumination. Two sets of electrodes (a) 30 μm / 15 μm and (b) 30 μm / 5 μm were investigated. I_{dark} means the current measured in the dark while $I_{\text{illumination}}$ represents the current measured under the illumination of 375 nm laser. (Average $R = 1 / \text{the slope of I-V curves}$) [14].
- Fig. 2.7** (a) One-dimensional array of resistors and nano-Schottky-diodes, where D1 represents the forward-biased Schottky diode, D2 the reverse-biased Schottky diode and R1 the resistance of Au NP. (b) (c) The models for nanodevice in dark and under illumination. For HSPICE simulation, Fowler-Nordheim diode model was employed, $V = 0.4 \text{ V}$, $R1 = 1 \text{ M}\Omega$, $R2 = 5 \text{ M}\Omega$ and $I = 5 \text{ pA}$ [14].
- Fig. 2.8** The cross sectional figures of two kinds of photo-sensing nanodevices on CMOS sensing

chip. (a) Au / AET-CdSe/ZnS nanodevice. (b) MSA-CdSe/ZnS / AET-CdSe/ZnS nanodevice.

Fig. 2.9 The schematic of CMOS sensing circuit.

Fig. 2.10 The HSPICE simulation results of CMOS sensing circuit (a)~(f).

Fig. 2.11 The simulation result of Output versus I_d , the resistance value of photo-sensing nanodevice is fixed to 7.5 k Ω . The linearity is 99.85% when the I_d ranging from 50 nA to 100 nA. When the I_d is upon 100 nA, the output will gradually saturate because M_{16} will leave the saturation region, entering triode region.

CHAPTER 3

Fig. 3.1 The flow diagram for preparing the Citrate-capped Au NPs solution.

Fig. 3.2 (a) The close photographs of 100 μ L of approximately 15 nm diameter Au NPs solution + 100 μ L DI water (left) and 100 μ L of approximately 5 nm diameter AET-CdSe/ZnS NPs solution + 100 μ L DI water (right). The Au NPs solution was in deep red while the AET-modified CdSe/ZnS NPs solution was in yellow. (b) The close photographs of the mixture of 100 μ L Au NPs solution and 100 μ L AET-modified CdSe/ZnS NPs solution just after mixing (right), the mixture after standing 6 hrs (middle) in room temperature, and the mixture after standing 5 days in room temperature (left). As we can see, the color of mixture just after mixing was like that of Au NPs solution. However, after 6 hrs, it became dark purplish red. After 5 days, there was obvious precipitate at the bottom and the supernatant became pale yellow.

Fig. 3.3 (a) The TEM image of Citrate-capped approximately 15 nm diameter Au NPs. (b) The TEM image of MSA-capped or AET-capped approximately 5 nm diameter CdSe/ZnS NPs. (c) The UV-visible spectrum of Au NPs solution. (d) The UV-visible and PL intensity spectrum of MSA-CdSe/ZnS or AET-CdSe/ZnS NPs solution.

Fig. 3.4 (a) The band gap and surface structure diagram of CdSe/ZnS NP. (b) The PL intensity spectrum of different kind of surface capping method of CdSe NP.

Fig. 3.5 The flow diagram for preparing the MSA-capped CdSe/ZnS NPs solution.

Fig. 3.6 The flow diagram for preparing the AET-capped CdSe/ZnS NPs solution.

Fig. 3.7 The overall fabrication process of the photo-sensing nanodevice by Coulombic force system on the silicon chip substrate is shown above. (a) The cross-section figure of the surface of the silicon chip designed for photo-sensing nanodevice fabrication, (b) The modification of TMSPEd on the silicon oxide surface and the protonation of amino ($-\text{NH}_3^+$) groups, (c) The assembly of \sim 15 nm diameter Au NPs or \sim 5 nm diameter MSA-CdSe/ZnS NPs on silicon oxide substrate by ionic interaction, (d) The assembly of \sim 5 nm diameter AET-CdSe/ZnS NPs on the silicon oxide substrate by ionic interaction, and (e) The formation of the photo-sensing nanodevice structures after repeated assembly process. (Not to scale)

CHAPTER 4

- Fig. 4.1** The environment setup for I-V characteristics measurement.
- Fig. 4.2** The environment setup for UV-visible absorbance spectrum measurement.
- Fig. 4.3** The environment setup for PL intensity spectrum measurement.
- Fig. 4.4** The layout of the CMOS sensing chip. The chip is $1460\ \mu\text{m} \times 1460\ \mu\text{m}$ and has 48 pins. There are eight identical CMOS sensing circuits at the corner part of the chip, and thirteen different size/shape electrodes at the center part of the chip.
- Fig. 4.5** The cross section figure of electrodes structure, where the four layers of metal lines ($\sim 10\ \mu\text{m}$ thickness) are connected by vias. The passivation window in this work is $86\ \mu\text{m} \times 86\ \mu\text{m}$. The silicon oxide region between Al electrodes has different shapes.
- Fig. 4.6** (a) The SEM image of the 13 electrodes. (b) The size (width * length between electrodes) figure of the corresponding 13 electrodes. The electrodes, (1)~(8), are connected to the eight identical CMOS sensing circuits. The rest five electrodes, E1~E5 are connected directly to pads for direct measurement.
- Fig. 4.7** The SEM images (100k magnification) of Au / AET-CdSe/ZnS nanostructure of different level construction are shown above (a)~(e).
- Fig. 4.8** The SEM images (100k magnification) of MSA-CdSe/ZnS / AET-CdSe/ZnS nanostructure of different level construction are shown above (a)~(e).
- Fig. 4.9** The overall experimental procedure of fabrication and measurement of photo-sensing nanodevice on TSMC $0.35\ \mu\text{m}$ silicon chip.
- Fig. 4.10** The SEM images of blank electrodes (a) $30\ \mu\text{m} \times 5\ \mu\text{m}$ electrodes (950 magnification), (b) $30\ \mu\text{m} \times 15\ \mu\text{m}$ electrodes (950 magnification), (c) The edge part of the electrodes (50k magnification).
- Fig. 4.11** The SEM images (70k magnification) of the edge part of Au / AET-CdSe/ZnS NPs modified electrodes. (a) 1-layered nanostructure, (b) 4-layered nanostructure, (c) 8-layered nanostructure, (d) 12-layered nanostructure.
- Fig. 4.12** The SEM images (70k magnification) of the edge part of MSA-CdSe/ZnS / AET-CdSe/ZnS NPs modified electrodes. (a) 1-layered nanostructure, (b) 4-layered nanostructure, (c) 6-layered nanostructure, (d) 12-layered nanostructure.
- Fig. 4.13** (a) The cross section figure of the electrodes structure corresponds to SEM image of the nanodevice–modified silicon chip. (b) The current flow trend of the electrodes structure, and the electrodes dominated the source of generated current. In the worse case, we must consider the whole chip area for calculation, not the area of the electrodes. (The twill line means the thin film structure composed of NPs)
- Fig. 4.14** The UV-visible absorption spectrum of multi-layered nanostructure on quartz glass. (a) Au / AET-CdSe/ZnS (b) MSA-CdSe/ZnS / AET-CdSe/ZnS. The Light Gray Line: 10% TMSPED/methanol \rightarrow quartz glass. The Black Line: 1-layered nanostructure. The Red Line: 2-layered nanostructure. The Green Line: 3-layered nanostructure. The Blue Line:

4-layered nanostructure. The Magenta Line: 5-layered nanostructure.

- Fig. 4.15** The PL emission spectrum of multi-layered nanostructures on quartz glass. (a)(c) The PL intensity of Au / AET-CdSe/ZnS and MSA-CdSe/ZnS / AET-CdSe/ZnS, 4-layered nanostructure. The Red Line: photo-excitation with 435nm wavelength; The Green Line: photo-excitation with 400 nm wavelength; The Blue Line: photo-excitation with 375 nm wavelength; The Black Line: photo-excitation with 365 nm wavelength. (b)(d) The PL intensity of Au / AET-CdSe/ZnS and MSA-CdSe/ZnS / AET-CdSe/ZnS, multi-layered nanostructure under 375 nm photo-excitation. The Black Line: 1-layered nanostructure; The Red Line: 2-layered nanostructure; The Green Line: 3-layered nanostructure; The Blue Line: 4-layered nanostructure; The Magenta Line: 5-layered nanostructure; The Yellow Line: 8-layered (b) and 6-layered (d) nanostructure; The Orange Line: 12-layered nanostructure.
- Fig. 4.16** The electrodes under measuring are shown above. Electrodes 1 and 2 have silicon oxide region of $30 \mu\text{m} * 15 \mu\text{m}$ and $30 \mu\text{m} * 5 \mu\text{m}$ (width * length), respectively.
- Fig. 4.17** The I-V curves of the multi-layered Au / AET-CdSe/ZnS photo-sensing nanodevice when in dark (black line) or illumination with 375 nm (blue line), 400 nm (green line), 435 nm (red line) laser diode.
- Fig. 4.18** (a) Two-dimensional array of resistors and nano-Schottky-diodes. (b) (c) The models for nanodevice in dark and under illumination. For HSPICE simulation, Metal-Insulator-Semiconductor diode model was employed, $V = 0.4 \text{ V}$, $R_1 = 0.25 \text{ M}\Omega$, $R_2 = 5 \text{ M}\Omega$ and $I = 5 \text{ pA}$.
- Fig. 4.19** The I-V curves of the multi-layered MSA-CdSe/ZnS / AET-CdSe/ZnS photo-sensing nanodevice when in dark (black line) or illumination with 375 nm (blue line), 400 nm (green line), 435 nm (red line) laser diode.
- Fig. 4.20** I-V characteristics of an illuminated solar cell. (a) Typical p-n junction solar cell in the fourth quadrant. (b) Au / AET-CdSe/ZnS solar cell in the second quadrant.
- Fig. 4.21** The electrodes of size $30 \mu\text{m} / X \mu\text{m}$ (width / length).
- Fig. 4.22** The measurement results of 4-layered, $30\mu\text{m} * 5\mu\text{m}$ electrodes, Au / AET-CdSe/ZnS nanodevice combined with CMOS sensing circuit are shown above (a)~(d), where I_d means the current following through the $R_d \sim 7.5\text{k}\Omega$. In this measurement, we fixed the $V_{\text{bias}} \sim 1.70118\text{V}$ and then illuminated with laser source or under dark condition.
- Fig. 4.23** The result of output versus I_d in both HSPICE simulation (dark line) and this measurement of photo-sensing circuit (red line). The power intensity of the laser diodes (375, 400, 435 nm) is $2.5\text{mW} / \text{cm}^2$

TABLE FOR FULL TEXT OF CHEMICAL REAGENTS

Simplified Form	Full Text (or Synonyms)	Formula	Molecular Weight
TMSPED	N-[3-(trimethoxysilyl)propyl]-ethylene diamine	$C_8H_{22}N_2O_3Si$	222.36
APTES	3-aminopropyltriethoxysilane	$C_9H_{23}NO_3Si$	221.37
Citric acid Monohydrate	Acidum citricum monohydricum	$C_6H_8O_7 \cdot H_2O$	210.14
Tyramine	4-(2-Aminoethyl)phenol	$C_8H_{11}NO$	137.18
MSA	D, L-mercaptosuccinic acid	$C_4H_6O_4S$	150.15
AET	2-aminoethane thiol	$C_2H_7NS.HCl$	113.61

